Molecular Neurobiology (2019) 56:7458–7472
https://doi.org/10.1007/s12035-019-1608-0

Critical Role of Monocyte Recruitment in Optic Nerve Damage Induced by Experimental Optic Neuritis

Marcos L. Aranda[1] · Diego Guerrieri[2] · Gonzalo Piñero[3] · María F. González Fleitas[1] · Florencia Altschuler[1] · Hernán H. Dieguez[1] · María I. Keller Sarmiento[1] · Mónica S. Chianelli[1] · Pablo H. Sande[1] · Damián Dorfman[1] · Ruth E. Rosenstein[1]

Received: 21 November 2018 / Accepted: 12 April 2019 / Published online: 1 May 2019

Abstract

Neuroinflammatory diseases are characterized by blood-brain barrier disruption (BBB) and leukocyte infiltration. We investigated the involvement of monocyte recruitment in visual pathway damage provoked by primary optic neuritis (ON) induced by a microinjection of bacterial lipopolysaccharide (LPS) into the optic nerve from male Wistar rats. Increased Evans blue extravasation and cellularity were observed at 6 h post-LPS injection. In WT-GFPþ/WT chimeric rat optic nerves, the presence of GFP(+) neutrophils and GFP(+) monocytes, and in wild-type rat optic nerves, an increase in $CD11b^{+}CD45^{low}$ and $CD11b^{+}CD45^{high}$ cell number, were observed at 24 h post-LPS. Gamma-irradiation did not affect the increase in BBB permeability, but significantly lessened the decrease in pupil light reflex (PLR), and retinal ganglion cell (RGC) number induced by LPS. At 6 h post-LPS, an increase in chemokine (C-C motif) ligand 2 (CCL2) immunoreactivity co-localized with neutrophils (but not microglia/macrophages or astrocytes) was observed, while at 24 h post-injection, an increase in Iba-1-immunoreactivity and its co-localization with CCL2 became evident. The co-injection of LPS with bindarit (a CCL2 synthesis inhibitor) lessened the effect of LPS on PLR, and RGC loss. The treatment with etoposide or gadolinium chloride that significantly decreased peripheral monocyte (but not neutrophil or lymphocyte) percentage decreased the effect of LPS on PLR, and RGC number. Moreover, a negative correlation between PRL and monocyte (but not lymphocyte or neutrophil) percentage was observed at 7 days post-LPS. Taken together, these results support that monocytes are key players in the initial events that take place during primary ON.

Keywords Optic nerve · Neuroinflammation · Blood-brain barrier · CCL2 · Monocytes

Introduction

Optic neuritis (ON), the most common optic neuropathy affecting young adults, involves inflammation, demyelination, and axonal injury in the optic nerve, which leads to retinal ganglion cell (RGC) loss and visual dysfunction [1]. The typical clinical presentation includes unilateral visual loss, afferent pupillary defect, abnormal visual evoked potentials (VEPs), and periocular or retro-orbital pain in association with eye movement. Vision loss is quite variable and ranges from mild to no light perception [1, 2]. Most patients show reduced contrast sensitivity and dyschromatopsia, which are often out of proportion to the visual acuity deficit. Although ON can be associated with neuromyelitis optica, multiple sclerosis (MS), and its validated experimental model, experimental autoimmune encephalomyelitis (EAE), the etiology varies, including inflammation, infections, toxic reasons, and genetic disorders [1, 2]. In most ON cases, the responsible etiology may not be known and in this case, it is termed idiopathic (or primary) ON

Electronic supplementary material The online version of this article (https://doi.org/10.1007/s12035-019-1608-0) contains supplementary material, which is available to authorized users.

✉ Ruth E. Rosenstein
ruthr@fmed.uba.ar

[1] Department of Human Biochemistry, Laboratory of Retinal Neurochemistry and Experimental Ophthalmology School of Medicine/CEFyBO, University of Buenos Aires/CONICET, Buenos Aires, Argentina

[2] Laboratory of Immunomodulators and ORGAN REGENERATION, School of Medicine/CEFyBO, University of Buenos Aires/CONICET, Buenos Aires, Argentina

[3] Department of Biological Chemistry and Institute of Chemistry and Biological Physicochemistry, School of Pharmacy and Biochemistry, University of Buenos Aires/CONICET, Buenos Aires, Argentina

[3]. Recently, we have developed a new experimental model of primary ON in rats through a single microinjection of bacterial lipopolysaccharide (LPS) directly into the optic nerve [4]. The microinjection of LPS induces a significant and persistent decrease in pupil light reflex (PLR) and VEP amplitude, as well as an increased optic nerve microglial/macrophage reactivity that are already evident at 24 h post-injection, without changes in the electroretinogram, signs of systemic inflammation, or cerebral involvement. In addition, astrocytosis, demyelination, and axon and RGC loss are observed at 21 days post-LPS microinjection [4]. These results support that the microinjection of LPS into the optic nerve may serve as an experimental model of primary ON. Neuroinflammatory diseases are characterized by blood-brain barrier (BBB) disruption and increased leukocyte infiltration. Circulating leukocytes that migrate to sites of tissue injury and infection are key players in inflammation by eliminating the primary inflammatory trigger and contributing to tissue repair [5–8]. Nevertheless, it has been well established that excessive or uncontrolled peripheral cell infiltration can cause enhanced tissue injury. In this line, it has been demonstrated that disruption of the BBB and immune cell infiltration is an early pathophysiological hallmark of MS and EAE which mediates demyelination and leads to axonal injury [9–12], and strategies aimed at preventing the recruitment of such immune cells can reduce axonal and myelin damage [11, 13]. In contrast, it has been shown that immune cell infiltration occurs after optic nerve demyelination in EAE mice [14]. Therefore, there is still no conclusive evidence to support a causal role for infiltrating peripheral immune cells in ON pathogenesis, and the contribution of leukocyte infiltration to ON initiation and development is yet to be defined. In this study, we investigated leukocyte recruitment in LPS-induced ON and its consequences on visual pathway damage.

Materials and Methods

Animals

Male Wistar rats (^{WT}Wistar) and homozygous fluorescent protein eGFP transgenic Wistar rats (^{eGFP}Wistar; Wistar-TgN (CAG-GFP) 184ys) (300 ± 50 g) were housed in a standard animal room with food and water ad libitum under controlled conditions of temperature (21 ± 2 °C), luminosity (200 lx), and humidity, under a 12-h light/12-h dark lighting schedule (lights on at 8:00 AM). A total number of 140 male ^{WT}Wistar were used for the experiments and they were distributed as follows: 20 animals for Evans blue experiments, 10 animals for hematoxylin and eosin (H&E) staining and immunohistochemical studies, 5 animals for chimeric rat generation, 20 animals for flow cytometry, 20 animals for irradiation, 15 animals for studies using recombinant tissue plasminogen activator (rtPA), 20 animals for bindarit treatment, and 30 animals for etoposide and gadolinium chloride treatment were used. In addition, a total number of 5 ^{eGFP}Wistar rats were used for chimeric rat generation.

Microinjections into the Optic Nerve

To induce experimental ON, animals were anesthetized with ketamine hydrochloride (150 mg/kg) and xylazine hydrochloride (2 mg/kg) intraperitoneally administered. Animal's head was shaved and the skin was disinfected with povidone-iodine (Pervinox). A lateral canthotomy was made to perform an incision of 2–3 mm. Lacrimal glands and extraocular muscles were dissected to expose 3 mm of the retrobulbar optic nerve under a surgical microscope. The optic nerve sheaths were opened longitudinally and a microinjection was performed with a 30G needle attached to a Hamilton syringe (Hamilton, Reno, NV, USA). The needle was inserted into the optic nerve as superficially as possible, 2 mm posterior to the globe, and 1 μl of 4.5 μg/μl *Salmonella typhimurium* LPS (Sigma Chemical Co., St Louis, MO, USA) in pyrogen-free saline, was injected for approximately 10 s. In the present study, vehicle-injected optic nerve served as the control group because in a previous study we found that vehicle injection per se did not affect optic nerve function and histology [4]. After injection, the skin incision was sutured and antibiotics were topically administered to prevent infection. In some experiments, rtPA (250 ng/μl, Actilyse®, Boehringer Ingelheim, Buenos Aires, Argentina) was microinjected into the optic nerve, following the procedure described for LPS microinjection, and in another set of experiments, bindarit (100 μM, Abcam Inc., Buenos Aires, Argentina) was co-injected with LPS.

Vascular Permeability

Vascular permeability was analyzed by albumin-Evans blue complex leakage from optic nerve vessels, as previously described [15, 16]. Briefly, animals were anesthetized and intrajugulary injected with a solution of Evans blue (2% wt/vol in phosphate buffer (PBS)). Immediately after injection, animals turned visibly blue, confirming the dye uptake and distribution. After 120 min, animals were deeply anesthetized and intracardially perfused with saline solution and optic nerves were obtained. Optic nerve microphotographs were obtained using identical exposure time, brightness, and contrast settings. For each group, results were qualitatively analyzed by comparing five optic nerves per group.

Histological Evaluation

Animals were deeply anesthetized and intracardially perfused with saline solution, followed by a fixative solution (4%

paraformaldehyde in PBS, pH 7.4). Eye cups and optic nerves were obtained from the optic nerve head to the optic chiasm and post-fixed in fixative solution for 24 h at 4 °C. After several washes, samples were dehydrated, cleared in butanol, and embedded in paraffin. Serial longitudinal and transversal sections (5 μm) were obtained using a microtome (Leica, Leica Microsystems, Buenos Aires, Argentina). Some sections were used for histological analysis (H&E staining). For each section, the average of four different sections was used as the representative value. Sections were mounted and viewed under an optic microscope (Nikon Eclipse E400, Tokyo, Japan). Light microscopic images (200×) were digitally captured via a Nikon Coolpix S10 camera (Nikon, Tokyo, Japan).

Optic Nerve Digestion and Flow Cytometry

Optic nerves were cut into small pieces and enzymatically digested in 500 μl of medium (DMEM, 10 mM HEPES, 16 μg/ml collagenase IV, 10 μg/ml DNase I, 5 mM Mg^{+2}, 2.5 mM Ca^{+2}) at 37 °C for 40 min with shaking (< 450 rpm). After adding one volume of PBS-EDTA (1 mM), the remaining tissue was mechanically disaggregated by successive passages through needles of decreasing caliber (18–21–23–25G) and filtered with a 70-μm mesh. Then, cells were centrifuged, washed, and stained with Zombie yellow viability dye according to the manufacturer's protocol (Biolegend, San Diego, CA, USA). Non-specific antibody binding was blocked by incubation for 10 min at room temperature in heat-inactivated rat serum diluted 1:1 in eFACS buffer (1 mM EDTA, 10% FCS). After washing, cells were incubated for 20–30 min at 4 °C with the following conjugated primary antibodies: Alexa™ 647 anti-rat CD45 and R-Phycoerythrin anti-rat CD11b), both from Biolegend. Finally, cells were washed, resuspended in 50 μl of PBS-EDTA, and immediately analyzed. All centrifugation steps were performed at 450 ×*g* for 5 min at 4 °C, and washes were done in eFACS buffer. At least 5×10^5 events per condition were analyzed in a Becton-Dickinson FACSAriaII™ flow cytometer (San Jose, CA, USA). Compensation controls were prepared with UltraComp eBeads™ (Thermo Fisher Scientific, Waltham, MA, USA) following the manufacturer's protocol. Using FlowJo v10.0.8 software (FlowJo, Ashland, OR, USA), doublets and dead cells were excluded, $CD45^+$ cells were gated out and plotted against CD11b in order to perform relative quantifications.

Immunohistochemical Studies

Antigen retrieval was performed by heating slices at 90 °C for 30 min in citrate buffer (pH 6.3). The following antibodies were used: a goat anti-ionized calcium-binding adaptor molecule 1(Iba-1) antibody (1:500; Abcam Inc., Buenos Aires, Argentina), a mouse monoclonal anti-glial fibrillary acidic protein (GFAP) antibody conjugated to Cy3 (1:1200; Sigma Chemical Co., St Louis, MO, USA), a rabbit polyclonal anti-chemokine (C-C motif) ligand 2 (CCL2) antibody (1:300; Abcam Inc., Buenos Aires, Argentina), a mouse monoclonal anti-CD3 antibody (1:200; Biolegend, San Diego, CA, USA), a mouse monoclonal anti-CD20 antibody (1:200; Abcam Inc., Buenos Aires, Argentina), a donkey anti-rabbit secondary antibody conjugated to Alexa 488 (1:500; Abcam Inc., Buenos Aires, Argentina), a donkey anti-mouse secondary antibody conjugated to Alexa 568 (1:500; Molecular Probes, Buenos Aires, Argentina), and a donkey anti-goat secondary antibody conjugated to Alexa 568 (1:500; Molecular Probes, Buenos Aires, Argentina). Sections were immersed in 0.1% Triton X-100 in 0.1 mol/l PBS for 10 min, incubated with 2% normal horse serum for 1 h for unspecific blockade, and then incubated overnight at 4 °C with the primary antibodies. After several washings, secondary antibodies were added, and sections were incubated for 2 h at room temperature. Regularly, some sections were treated without the primary antibodies to confirm specificity. For each nerve, results obtained from four separate regions were averaged, and the mean of five nerves was recorded as the representative value for each group. For RGC immunodetection, retinas were carefully detached and flat-mounted with the vitreous side up in superfrost microscope slides (Erie Scientific Company, Portsmouth, New Hampshire, USA). Whole-mount retinas were incubated overnight at 4 °C with a goat anti-Brn3a antibody (1:500; Santa Cruz Biotechnology, Buenos Aires, Argentina). After several washes, a donkey anti-goat secondary antibody conjugated to Alexa 568 (1:500; Molecular Probes, Buenos Aires, Argentina) was added, and incubated for 2 h at room temperature. Finally, retinas were mounted with fluorescent mounting medium (Dako, Glostrup, Denmark) and observed under an epifluorescence microscope (BX50; Olympus, Tokyo, Japan) connected to a video camera (3CCD; Sony, Tokyo, Japan) attached to a computer running image analysis software (Image-Pro Plus; Media Cybernetics Inc., Bethesda, MD, USA). For each retina, results obtained from eight separate quadrants (four from the center and four from the periphery) were averaged, and the mean of five eyes was recorded as the representative value. Immunofluorescence studies were performed by analyzing comparative digital images from different samples by using identical exposure time, brightness, and contrast settings.

Morphometric Analysis

All the images obtained were assembled and processed using Adobe Photoshop CS5 (Adobe Systems, San Jose, CA, USA) to adjust brightness and contrast. No other adjustments were made. For all morphometric image processing and analysis, digitalized captured TIFF images were transferred to ImageJ

software (National Institutes of Health, Bethesda, Maryland; http://imagej.nih.gov/ij/).

Pupillary Light Reflex

Animals were dark-adapted for 2 h. The eye in which the nerve was injected was stimulated with high-intensity light (1200 lx) for 30 s, and PRL was recorded in the contralateral (intact) eye (i.e., consensual PLR). The recordings were made under infrared light with a digital video camera (Sony DCR-SR60, Tokyo, Japan) as previously described [14, 16]. The sampling rate was 30 frames per second. Images were acquired with OSS Video Decompiler Software (One Stop Soft, New England, USA). The results were expressed as the percentage of the pupil contraction before (steady state) and 30 s after the light pulse.

Bone Marrow Depletion by Gamma Irradiation

Animals were anesthetized as described above. Whole-body gamma irradiation at 87.2 rad/s was performed in an IBL 437C irradiator (^{137}Cesium), manufactured by MikRon Inc. (Wareham, MA, USA) in CEBIRSA (Buenos Aires, Argentina). The total irradiation dose was 9600 rads. During irradiation, animals' heads were covered with a 5-mm thick lead protective helmet. Irradiation was performed at 2 days before vehicle, LPS, or rtPA injection (Fig. 1). The irradiation protocol was performed as previously described [17].

Generation of Chimeric Rats

^{WT}Wistar rats were anesthetized and irradiated as described above. The next day, ^{eGFP}Wistar rats were euthanized and bone marrow cells were harvested from the femur and tibia. Bone marrow cells (5×10^5 cells) were injected via the jugular vein in irradiated ^{WT}Wistar rats. Four weeks after, the presence of GFP(+) leukocytes in blood samples from WT-GFPp/WT chimeric rats were analyzed by blood smears and flow cytometry (BD Accuri™ C6 Plus in FL1 channel). At 6 weeks, rats were injected with vehicle or LPS in the optic nerve while the contralateral optic nerve remained intact. Animals were euthanized at 1 day post-injection of vehicle or LPS for histological evaluation.

Etoposide and Gadolinium Chloride Treatments

Animals were intraperitoneally injected with etoposide (2 mg/kg, Microsules, Buenos Aires, Argentina) at days −3, −2, −1, 0, 2, 4, and 6 post-LPS), or gadolinium chloride (5 mg/kg in 0.6% NaCl, Sigma Chemical Co., St Louis, MO, USA) at days −1, 0, 2, 4, and 6 post-LPS, or vehicle (0.9% NaCl), as shown in Fig. 1. Blood samples were obtained from the tail vein at 0, 4, 7, and 21 days post-injection, and leukocyte populations were analyzed by flow cytometry (BD Accuri™ C6 Plus). Results were expressed as percentage of total counts. PLR was measured at 7 and 21 days post-injection, and a total of 15 animals (five animals per treatment) were euthanized at 21 days post-injection of vehicle or LPS for histological evaluation.

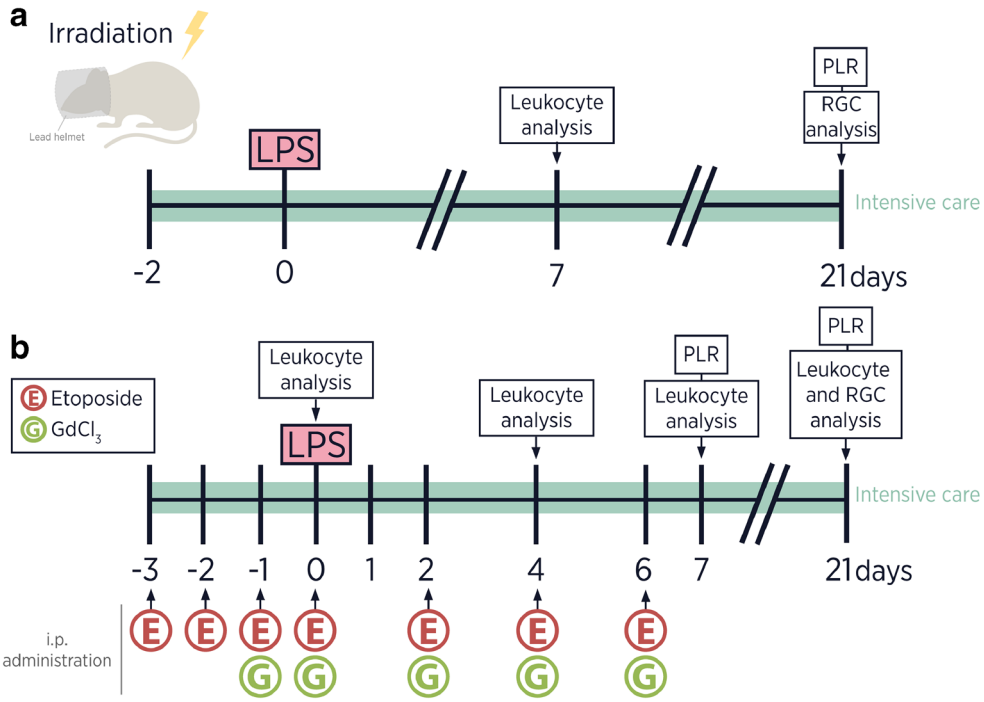

Fig. 1 Time-line diagrams for experimental procedures. Panel **A**: Animals were irradiated at 2 days before vehicle, LPS, or rtPA injection. During irradiation, animals' heads were covered by a lead protective helmet. At 7 days post-LPS, blood samples were analyzed by flow cytometry, while PLR was analyzed at 21 days post-injection. Panel **B**: animals were intraperitoneally injected with etoposide (E) or gadolinium chloride (G). Leukocyte populations were analyzed at 0, 4, 7, and 21 days post-LPS, and PLR was assessed at 7 and 21 days post-injection. At 21 days post-injection, animals were sacrificed and RGC number was analyzed

Statistical Analysis

Animals were assigned randomly to various experimental groups (using a random number generator: http://www.randomizer.org/form.htm). The data collected was processed randomly and appropriately blocked. Experimenters were blind to group and outcome assignment, and an appropriate sample size was computed when the study was being designed. Statistical analysis of results was performed by one- or two-way analysis of variance (ANOVA), followed by Tukey's test. Significance was set at P values below 0.05 for all analyses, and values are expressed as mean ± standard error (SE).

Results

In order to analyze the effect of experimental ON on BBB integrity, Evans blue was intravenously administered to naïve animals or animals in which one optic nerve was injected with vehicle and the contralateral optic nerve received LPS. In naïve and vehicle-injected optic nerves, the dye was exclusively observed within the vessel lumen, with very low background fluorescence levels. In LPS-injected optic nerves, a generalized leakage of the Evans blue-albumin complex was observed already at 6 h, and persisted at 24 h and 7 days post-injection (Fig. 2A). In addition, focal dye leakages from superficial vessels were observed in LPS-injected optic nerves at 24 h post-LPS (Fig. 2B). To assess cellularity, optic nerve longitudinal sections were stained with H&E (Fig. 3A). Nucleus number was increased in LPS-injected optic nerves as early as 6 h, and persisted at 24 h post-injection, as compared with vehicle-injected optic nerves. To dissect the contribution of peripheral leukocyte infiltration versus resident immune cells, WT-GFPþ/WT chimeric rats were developed (Fig. 3B, C). In addition, flow cytometry studies were performed in wild type Wistar rats, as shown in Fig. 3D. GFP(+) neutrophils and GFP(+) monocytes were observed in LPS-injected optic nerve longitudinal sections from WT-GFP^{+} → WT chimeric rats (Fig. 3C), whereas no GFP(+) cells were identified in vehicle-injected optic nerves. The presence of T or B cells in the optic nerve was not evident at 24 h post-LPS, as demonstrated by the absence of immunoreactivity for CD3 and CD20, respectively (data not shown). LPS injection induced a significant increase in the number of CD11b^{+}CD45^{low} (microglia) cells at 6 h and 24 h post-LPS, while the number of CD11b^{+}CD45^{high} (macrophage) cells significantly increased at 24 h (but not 6 h) post-injection. To analyze the influence of leukocyte infiltration on optic nerve damage induced by experimental ON, ^{WT}Wistar rats bearing a lead shield to protect their heads and eyes were gamma-irradiated, and 2 days after irradiation, animals were injected with vehicle in one optic nerve and LPS in the contralateral optic nerve. Irradiation did not affect the increase in BBB permeability at 6 h post-

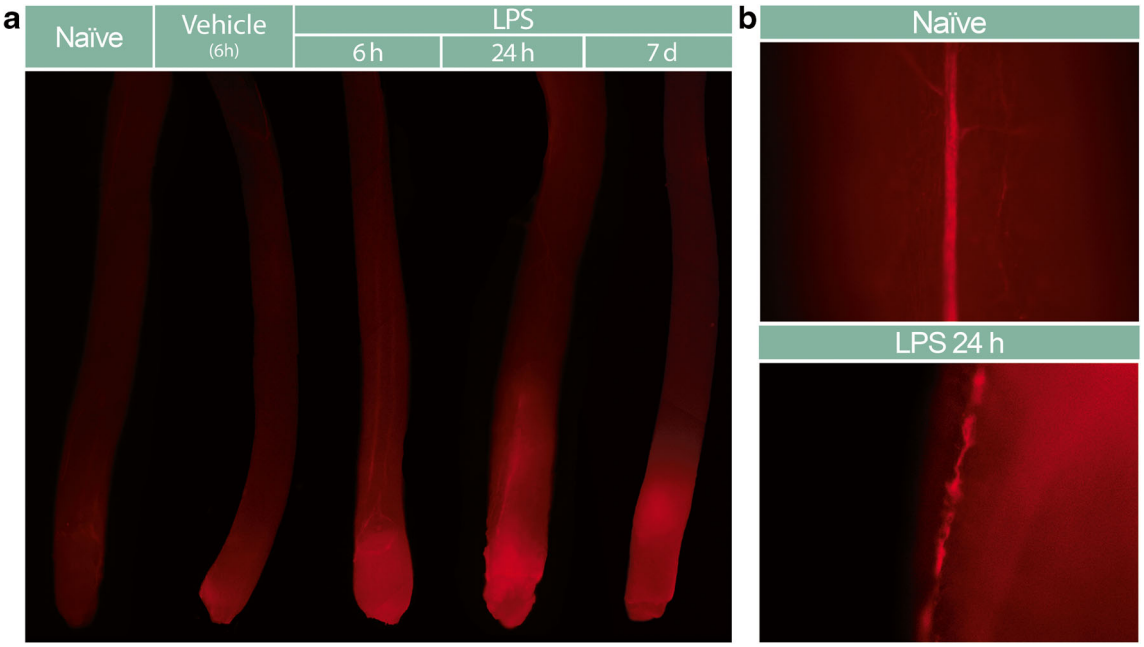

Fig. 2 Effects of LPS on BBB permeability. Representative epifluorescent images of naïve, vehicle- or LPS-injected optic nerves after intravascular perfusion with Evans blue. Shown are images representative of five optic nerves per group. Panel **A**: In naïve and vehicle-injected optic nerves, the dye was exclusively observed within the vessel lumen, with very low background fluorescence levels. In LPS-injected optic nerves, a generalized leakage of the Evans blue-albumin complex was observed already at 6 h and persisted at 24 h and 7 days post-injection. Panel **B**: superficial optic nerve vessels from naïve or LPS-injected animals at 24 h post-injection. Note focal dye leakages in LPS-injected optic nerves that were not observed in intact optic nerves

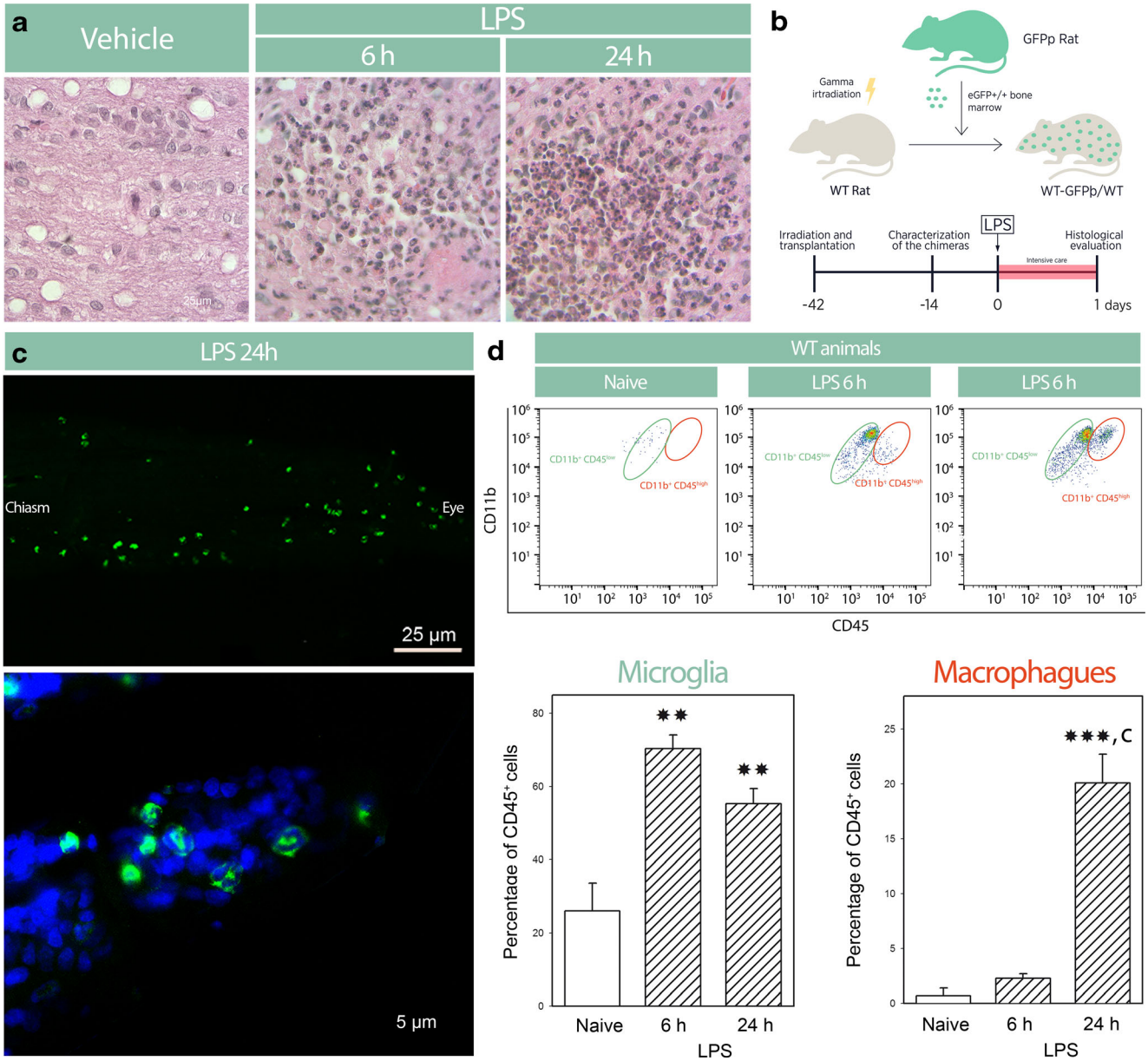

Fig. 3 Effect of LPS on optic nerve cellularity. Panel **A**: optic nerve longitudinal sections stained with H&E from vehicle or LPS-injected animals at 6 and 24 h post-injection. An increased nucleus number was detected in LPS-injected optic nerves as early as 6 h, and persisted at 24 h post-injection, as compared with vehicle-injected optic nerves. Panel **B**: Schematic representation of WT-GFP^{+} → WT chimeric rat generation. Panel **C**: Optic nerve longitudinal sections from WT-GFP^{+} → WT chimeric rats at 24 h post-LPS showing the presence of GFP(+) neutrophils, and GFP(+) monocytes viewed with low (upper panel) and high (lower panel) magnification (arrow: neutrophils, arrowhead: monocytes). Panel **D**: Microglia (CD11b^{+}CD45^{low}) and macrophage (CD11b^{+}CD45^{high}) analysis by flow cytometry in wild type rats. LPS injection induced a significant increase in the number of CD11b^{+}CD45^{low} (microglia) cells at 6 h and 24 h post-LPS, while the number of CD11b^{+}CD45^{high} (macrophage) cells significantly increased at 24 h (but not 6 h) post-injection. Data are the mean ± SEM ($n = 5$ animals per group). One-way ANOVA, microglia: $F_{interaction\ (2,12)}$, 17.32; macrophages: $F_{interaction\ (2,12)}$, 46.95; $^{**}P < 0.001$, $^{***}P < 0.001$ vs. naïve animals, c: $P < 0.001$ vs. 6 h post-LPS, by Tukey's test

injection (Fig. 4A), but lessened the decrease in PLR (Fig. 4B) and Brn3a(+) RGC number (Fig. 4C) induced by LPS at 21 days post-injection. Tissue-type plasminogen activator (tPA) is a serine protease well known to promote fibrinolysis; however, it has been shown that independently of its thrombolytic activity, tPA can directly affect BBB integrity [18–23]. Therefore, in order to further analyze the consequences of BBB disruption and leukocyte recruitment, rtPA was microinjected into the optic nerve. At 6 h post-injection, rtPA increased BBB permeability (Fig. 5A), and at 21 days post-injection, rtPA significantly decreased PLR (Fig. 5B) and Brn3a(+) RGC number (Fig. 5C). Animal irradiation lessened the effect of rtPA on light-induced pupil constriction and Brn3a(+) RGC number (Fig. 5A, B, respectively).

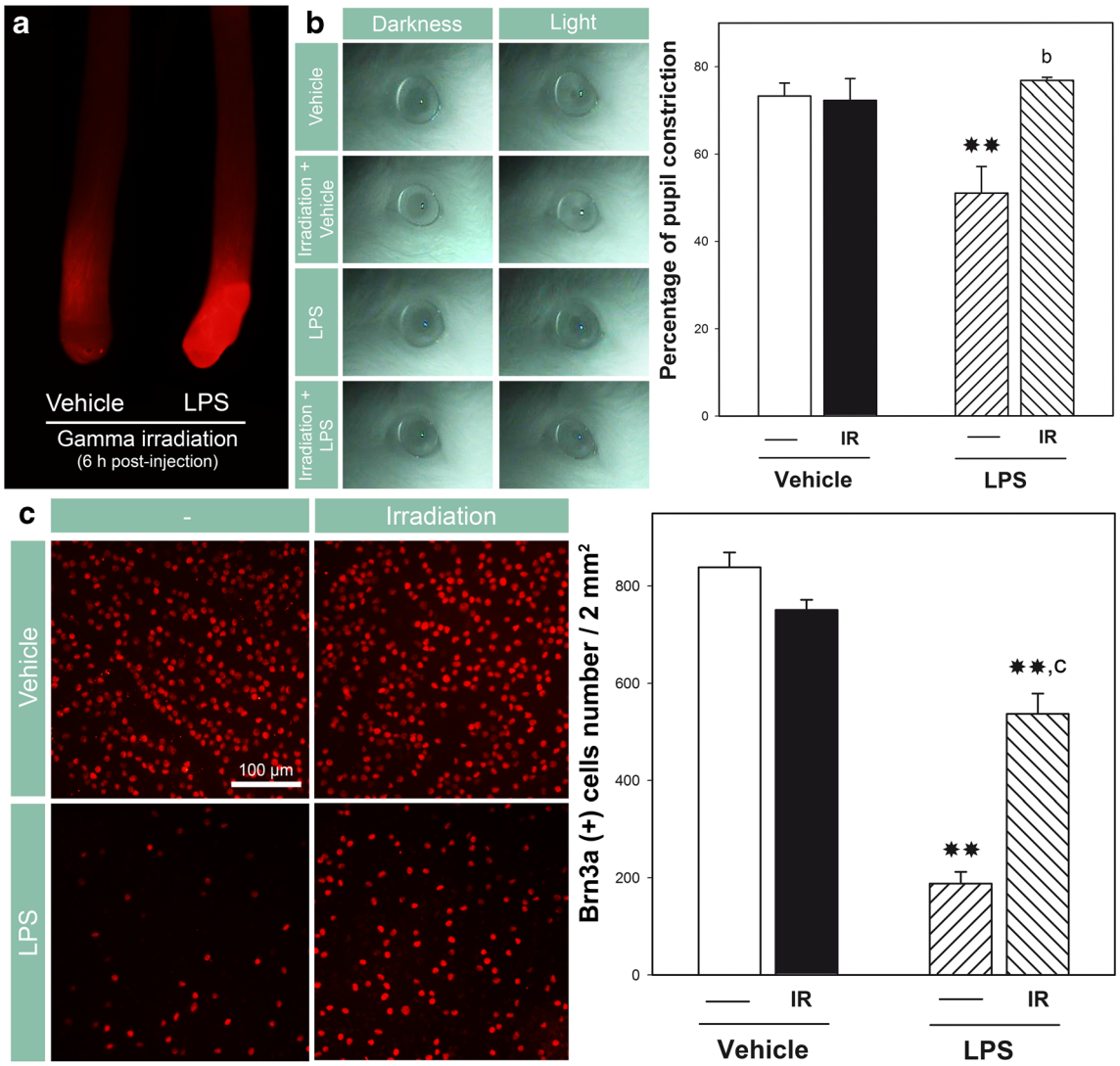

Fig. 4 Effect of LPS and irradiation on optic nerve damage induced by experimental ON. Panel **A**: optic nerve BBB permeability analysis by Evans blue perfusion. Irradiation did not affect the increase in BBB permeability induced by LPS at 6 h post-injection. Shown are images representative of five optic nerves per group. Panel **B**: The pupil diameter (relative to the limbus diameter) was measured at 21 days after vehicle or LPS injection into the optic nerve from non-irradiated or irradiated animals, and the percentage of pupil constriction was calculated in the contralateral eye whose optic nerve remained intact. In non-irradiated animals, LPS induced a significant decrease in the average of pupillary constriction in response to a light flash (1200 lx), while irradiation completely prevented the effect of LPS on PLR. Panel **C**: Effect of irradiation and LPS injection on RGCs number. Representative photomicrographs of Brn3a-immunostaining in flat-mounted retinas whose optic nerves from non-irradiated or irradiated animals were injected with vehicle or LPS. In non-irradiated animals, LPS injection induced a significant decrease in Brn3a(+) RGC cell number, while irradiation significantly decreased the effect of LPS on this parameter. Data are the mean ± SEM ($n = 5$ animals per group). Two-way ANOVA, panel **B**: $F_{\text{interaction (2,24)}}$, 7.43 $P < 0.01$; panel **C**: $F_{\text{interaction (2,24)}}$, 25.03 $P < 0.001$. $^{**}P < 0.01$, vs. vehicle-injected optic nerves from non-irradiated animals; b: $P < 0.01$, c: $P < 0.001$ vs. LPS-injected optic nerves from non-irradiated animals, by Tukey's test

Chemokines play crucial roles in leukocyte trafficking into the CNS. At 6 h post-LPS, an increase in CCL2-immunoreactivity that co-localized with cells morphologically similar to neutrophils, but not microglia/macrophages (Iba-1(+) cells) or astrocytes (GFAP(+) cells), was observed in longitudinal optic nerve sections (Fig. 6). Notably, LPS decreased GFAP-immunoreactivity and did not affect Iba-1-immunostaining at 6 h post-LPS, while at 24 h post-injection, an increase in Iba-1-immunoreactivity and its co-localization with CCL2 became evident (Fig. 6). The co-injection of LPS with bindarit (a CCL2 synthesis inhibitor) which decreased CCL2 levels in the optic nerve at 6 h post-injection (Fig. 7A) significantly lessened the effect of LPS on PLR (Fig. 7B), and Brn3a(+) RGC loss at 21 days post-injection (Fig. 7C). Etoposide and gadolinium chloride are chemotherapeutic agents able to deplete circulating monocytes [24, 25]. The effect of irradiation, etoposide (injected at days − 3, − 2, − 1, 0, 2, 4, and 6 post-LPS), or gadolinium chloride (injected at days −1,

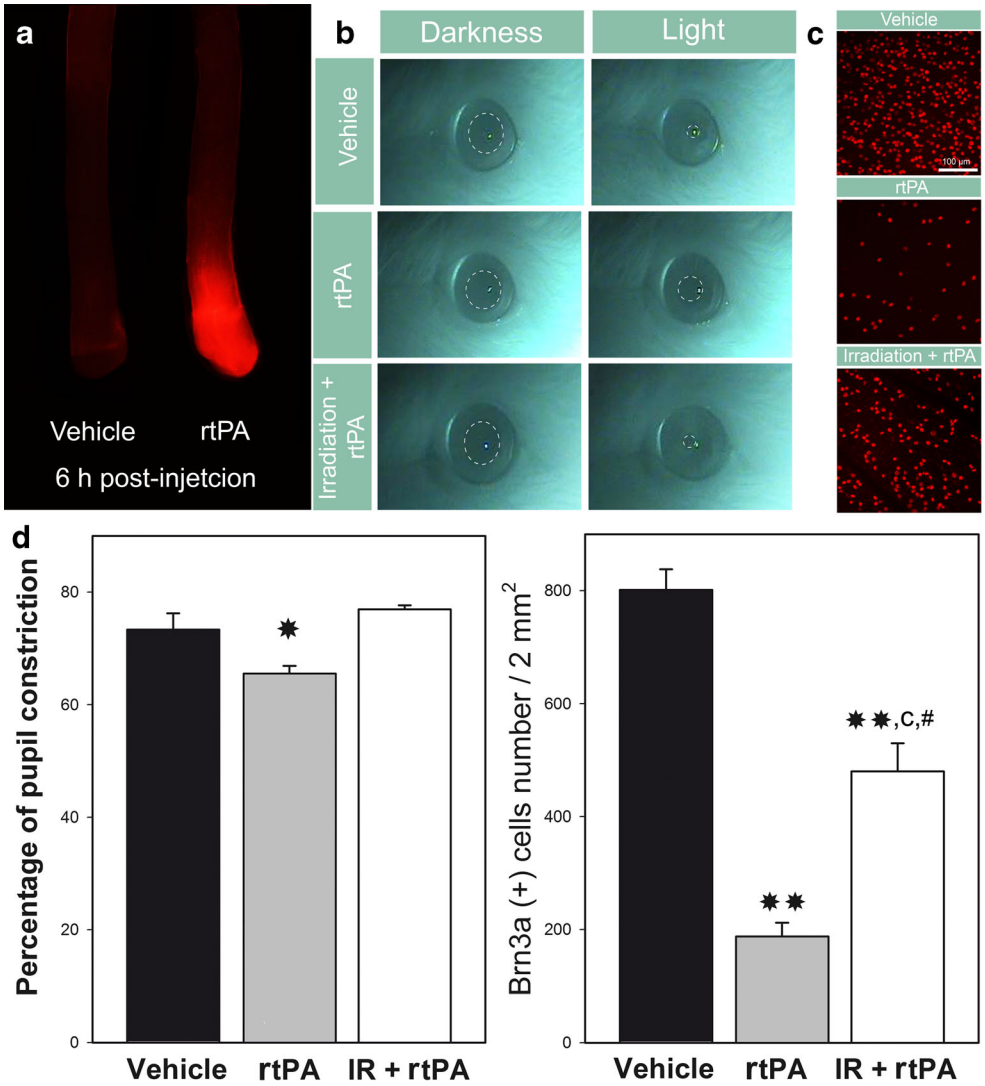

Fig. 5 Effect of rtPA and irradiation on experimental ON. Panel **A**: rtPA increased optic nerve BBB permeability at 6 h post-injection. Shown are images representative of five optic nerves per group. Panel **B**: Representative images of the consensual PLR (i.e., the pupil contraction of one eye, when the contralateral eyes was stimulated with light). Panel **C**: Representative photomicrographs of Brn3a-immunostaining in flat-mounted retinas. Panel **D**: Quantification of light-induced pupil constriction percentage, and Brn3a(+) RGC number. In non-irradiated animals, rtPA significantly decreased PLR, and RGC number at 21 days post-injection, while irradiation lessened the effect of rtPA on these parameters. Data are the mean ± SEM ($n = 5$ animals per group). Two-way ANOVA, panel **B**: $F_{interaction\ (2,24)}$, 7.43 $P < 0.01$; panel **C**: $F_{interaction\ (2,24)}$, 25.03 $P < 0.001$. *$P < 0.05$, **$P < 0.01$, vs. vehicle-injected optic nerves; c: $P < 0.001$ vs. rtPA-injected optic nerves; #: $P < 0.05$ vs. rtPA-injected optic nerves from non-irradiated animals, by Tukey's test

0, 2, 4, and 6 post-LPS) on monocyte, neutrophil, and lymphocyte percentage in naïve, vehicle (instead of etoposide or gadolinium chloride), or LPS-injected animals, at days 0, 4, 7, and 21 post-injection is depicted in Table 1. The effect of irradiation on leukocyte number was only assessed at 7 days post-injection to minimize the manipulation of immune-suppressed animals. The treatment with etoposide or gadolinium chloride that significantly decreased peripheral monocyte (but not neutrophil or lymphocyte) percentage at days 0, 4, and 7 (but not 21) post-LPS (Table 1) significantly decreased the effect of LPS on PLR (Fig. 8A, and Online Resource 1), and RGC number (Fig. 8B, and Online Resource 1) at 21 days post-LPS. Figure 8C shows a correlation between monocyte, lymphocyte, and neutrophil percentage and the consensual PLR at 7 days post-LPS. A negative correlation between PRL and monocyte (but not lymphocyte or neutrophil) percentage was evident.

Discussion

The present results support that monocyte recruitment into the optic nerve plays a critical role in the visual pathway damage induced by experimental primary ON in male rats. ON induced by LPS microinjection into the optic nerve provoked

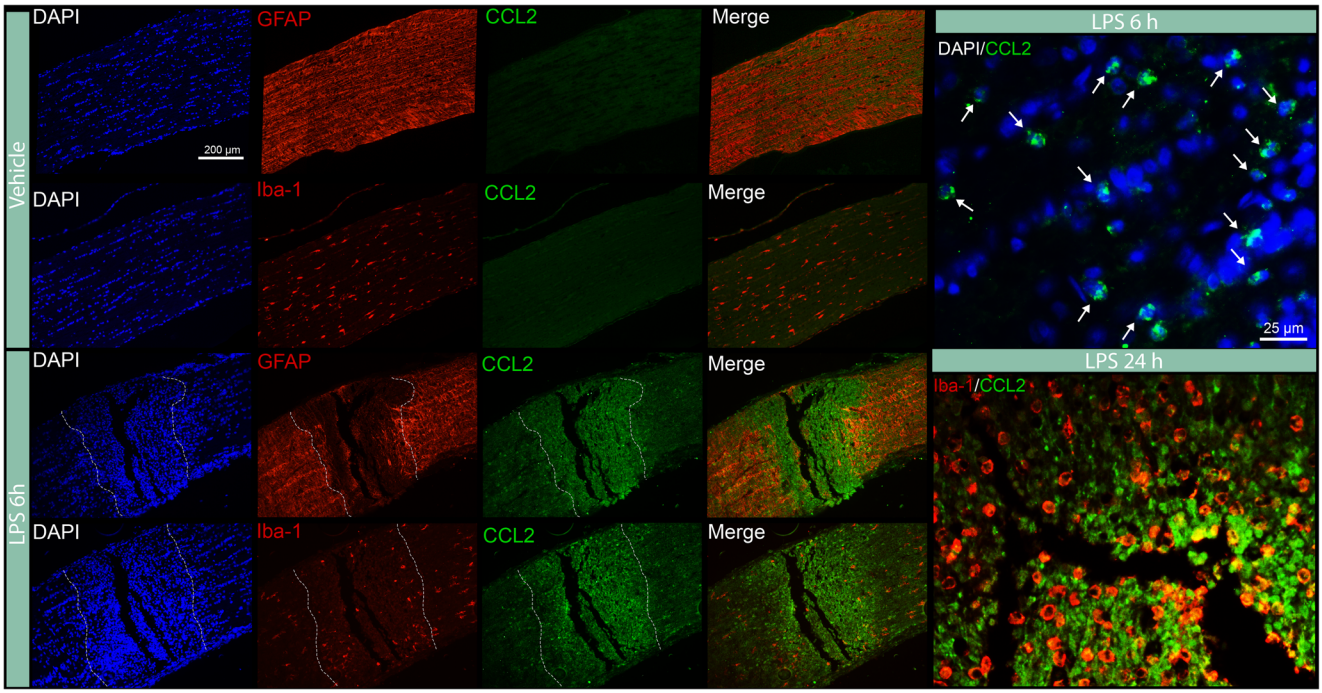

Fig. 6 Effect of LPS on CCL2-immunoreactivity in the optic nerve. Representative photomicrographs showing Iba-1-, GFAP-, and CCL2-immunoreactivity in optic nerve longitudinal sections. Shown are images representative of five optic nerves per group. An increase in CCL2-immunoreactivity co-localized with cells morphologically similar to neutrophils (white arrows), but not with microglia/macrophages or astrocytes was observed at 6 h post-LPS. LPS decreased GFAP-immunoreactivity and did not affect Iba-1-immunostaining at 6 h post-injection, while at 24 h, an increase in Iba-1-immunoreactivity and its co-localization with CCL2 became evident (white arrows)

BBB disruption, and increased cellularity, which were already evident at 6 h post-injection. In the CNS, innate immune surveillance is mainly coordinated by microglia. These CNS resident myeloid cells are assumed to help orchestrate the immune response against brain infections [26]. In LPS-induced ON, the increase in Iba-1-immunoreactivity starts at 24 h (but not 6 h) and persists until day 21 post-injection [4]. Iba-1 is expressed in microglia and monocyte-derived macrophages which are morphologically indistinguishable from each other. A commonly used non-genetic approach to discern microglia from recruited monocyte-derived cells during disease consists in generating GFP bone marrow chimeras. As shown herein, the presence of GFP(+) neutrophils and GFP(+) monocytes was observed at 24 h post-LPS, a time point at which an increase in the number of both $CD11b^{+}CD45^{low}$ and $CD11b^{+}CD45^{high}$ cells was shown by flow cytometry studies in wild-type animals. It should be noted that flow cytometry studies revealed an increase in $CD11b^{+}CD45^{low}$ (microglia) cell number at 6 h post-LPS, which was not observed by immunohistochemical labeling of Iba-1, a conspicuous marker for microglia/macrophages. Currently, the reasons for this discrepancy are not clear. However, it seems likely that a different sensitivity and the use of different markers for each one of these assays could account for it. Taken together, these results suggest that at 6 h post-injection, the increased cellularity could be attributed to infiltrated neutrophils and $CD11b^{+}CD45^{low}$ cells, while at 24 h post-LPS, a mixed contribution of neutrophils, monocyte-derived macrophages, and microglial cell proliferation could increase cell number in the optic nerve. In the spinal cord of EAE mice, neutrophils are among the first inflammatory cells recruited into the CNS [9], and monocyte-derived macrophages constitute the largest proportion of cells identified in inflammatory infiltrates in the optic nerve during all stages of EAE-ON [27]. In addition, it has been demonstrated that LPS induces an early recruitment of neutrophils in the CNS [28] and that the depletion of peripheral blood monocytes attenuates neuroinflammation induced by LPS injection [29]. In contrast with our results, it has been shown that in EAE-ON, microglial cell activation occurs well ahead of leukocyte infiltration [30], suggesting that the course of ON may vary depending on the induction mechanism of the disease. EAE-ON that involves an immune-mediated demyelination process differs from LPS-induced ON in several aspects [4]. Therefore, it seems not surprising to find also differences between these experimental models regarding the events involved in the course of the experimental disease.

The hypothesis that LPS-induced monocyte recruitment contributed to the visual pathway damage was supported by the fact that a single dose of gamma-irradiation before LPS microinjection that significantly decreased peripheral monocyte, neutrophil, and lymphocyte percentage, robustly decreased the effect of ON on PLR and RGC number. It has been demonstrated that neutrophil depletion leads to a marked

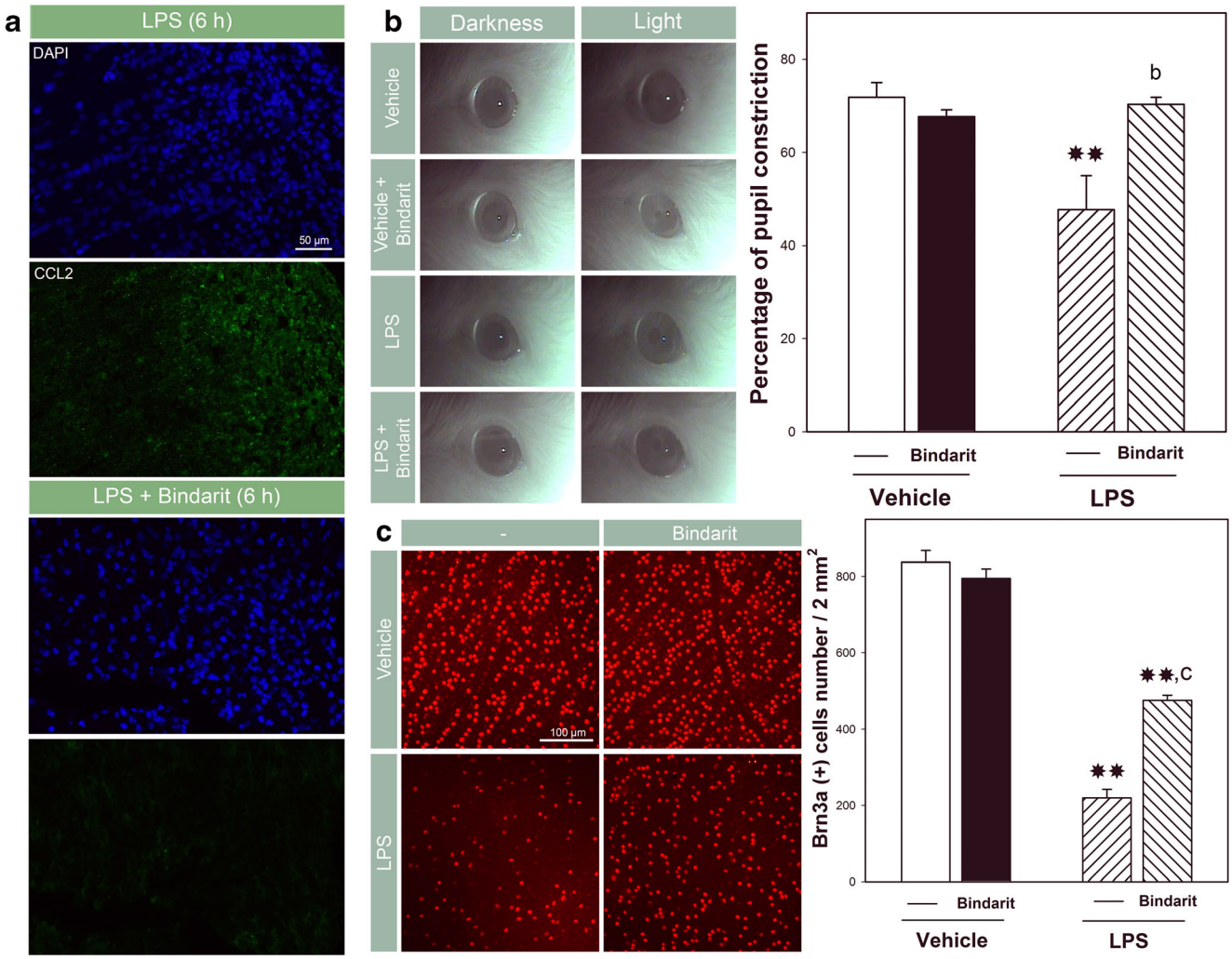

Fig. 7 Effect co-injection of LPS with bindarit on damage induced by experimental ON. Panel **A**: Representative photomicrographs showing CCL2-immunoreactivity in longitudinal sections of optic nerves that received LPS or LPS + bindarit, at 6 h post-injection. Shown are images representative of five optic nerves per group. Bindarit that showed no effect in vehicle-injected optic nerves, avoided the up-regulation of CCL2 induced by LPS. Panel **B**: Representative images of the consensual PLR and quantification of pupil constriction percentage. Bindarit completely avoided the effect of LPS on PRL at 21 days post-injection. Panel **C**: Representative photomicrographs of Brn3a-immunoreactivity in flat-mounted retinas and quantification of Brn3a(+) RGC number. Bindarit significantly avoided RGC loss induced by LPS. Data are the mean ± SEM ($n = 5$ animals per group). Two-way ANOVA, *PLR*: $F_{\text{interaction (1,16)}}$, 10.74 $P < 0.01$; *Brn3a(+)*: $F_{\text{interaction (1,16)}}$, 40.58 $P < 0.001$. $^{**}P < 0.01$, vs. vehicle-injected optic nerves; b: < 0.01: c: $P < 0.001$ vs. LPS-injected optic nerves, by Tukey's test

decrease in vascular leakage in the spinal cord from EAE mice [9]. In contrast, in our experimental setting, LPS provoked an increase in BBB permeability even in irradiated animals, supporting that BBB integrity loss per se was not enough to induce visual pathway damage, and that the early LPS-induced disruption of the BBB in the optic nerve did not depend on peripheral cell infiltration, but likely on local processes. The exact mechanisms by which LPS injection in the optic nerve cause BBB disruption remain under investigation. It has been shown that LPS induces various cytokines and other inflammatory mediators, which contribute to disruption of the BBB [31, 32]. We have previously shown that LPS injection into the optic nerve provokes an increase in nitric oxide synthase 2, cyclooxygenase-2, interleukin-1β, and TNFα levels [33, 34]. Therefore, without excluding the involvement of other mechanisms [31], it is tempting to speculate that these inflammatory signals could account for the BBB disruption induced by LPS. The involvement of BBB disruption and leukocyte recruitment in visual pathway damage was also demonstrated through a single microinjection of rtPA into the optic nerve. As already mentioned, rtPA can degrade the BBB likely through an increase in matrix metalloproteinases, without degradation of the vascular basement membrane [18, 19], and as such, rtPA was used to induce a sterile BBB disruption, and subsequent peripheral blood cell infiltration [20–23]. Consistently with the effect of LPS, rtPA microinjected into the optic nerve induced a significant decrease in PLR and RCG number at 21 days post-injection.

Table 1 Effect of irradiation, etoposide, and gadolinium chloride on lymphocyte, monocyte, and neutrophil percentage

Parameter	Treatment	0 days post-injection	4 days post-injection	7 days post-injection	21 days post-injection
Lymphocytes	Naïve			10.01 ± 0.78	
	Vehicle			9.90 ± 0.81	
	Irradiation			3.94 ± 1.91**	
	Etoposide	8.38 ± 2.45	14.92 ± 0.43	15.60 ± 2.18	6.88 ± 3.50
	$GdCl_3$	2.80 ± 0.05	16.95 ± 6.32	18.50 ± 1.91	15.23 ± 2.75
Monocytes	Naïve			3.21 ± 0.48	
	Vehicle			3.01 ± 0.30	
	Irradiation			0.77 ± 0.20 **	
	Etoposide	0.55 ± 0.20**	0.75 ± 0.22**	1.80 ± 0.20*	5.66 ± 0.55**
	$GdCl_3$	0.24 ± 0.07**	1.50 ± 0.10*	1.60 ± 0.40*	5.68 ± 0,60**
Neutrophils	Naïve			2.97 ± 0.32	
	Vehicle			3.10 ± 0.40	
	Irradiation			1.07 ± 0.40**	
	Etoposide	3.77 ± 1.82	2.10 ± 0.47	3.61 ± 1,47	1.51 ± 0.55
	$GdCl_3$	2.62 ± 1.37	1.92 ± 0.60	3.74 ± 1.13	1.99 ± 0.73

Blood samples from irradiated animals were obtained at 7 days post-injection of LPS. Blood samples from etoposide- and gadolinium chloride-treated animals were obtained at 0, 4, 7, and 21 days post-injection of LPS. Data are the mean of total count percentage ± SEM ($n = 5$ animals per group). One way ANOVA, Monocytes (irradiation): $F_{interaction\ (4,4)}$, 4.76 $P < 0.01$; Monocytes (etoposide): $F_{interaction\ (4,20)}$, 33.62 $P < 0.001$; Monocytes (gadolinium chloride): $F_{interaction\ (4,20)}$, 28.62 $P < 0.001$; Lymphocytes (irradiation): $F_{interaction\ (4,4)}$, 5.99 $P < 0.05$; Neutrophils (irradiation): $F_{interaction\ (4,4)}$, 1.56 $P < 0.01$i *$P < 0.05$, **$P < 0.01$, vs. naïve animals, by Tukey's test

Although it has been demonstrated that rtPA activates microglia [35, 36] and induces excitotoxic neuronal degeneration [36–39], the present results support that the effect of rtPA on the visual pathway could be attributable not only to BBB disruption but also to leukocyte infiltration, as shown by the fact that irradiation significantly decreased the effect of rtPA on PLR and RGC number at 21 days post-rtPA. Glaucoma and ON are the two major degenerative causes of optic nerve damage [39], and a common feature of these optic neuropathies is RGC loss and axonal damage. It has been shown that radiation protects from glaucoma by preventing the entry of monocytes into the eye [40], supporting another common feature between these neuropathies.

The chemokine CCL2 (formerly called Monocyte Chemoattractant Protein 1) is a critical mediator of inflammation in several neuroinflammatory diseases, including MS, EAE [41], and Alzheimer's disease [42], among many others. Although its precise mechanism of action remains to be elucidated, it has been demonstrated that CCL2 stimulates monocyte migration into the CNS [43–46] and induces microglial cell proliferation [47]. LPS induces CCL2 upregulation in the rat brain [48, 49], hypothalamus [50], and retina [51], as well as CCL2 secretion by neutrophils [52]. In this line, an increase in CCL2-immunoreactivity co-localized with neutrophils, but not with Iba-1(+) cells, or astrocytes was observed at 6 h post-LPS, while at 24 h, a co-localization of Iba-1(+) cells (microglia/macrophages) and CCL2 was evident. It has been demonstrated that global knockout [53] or antibody depletion of CCL2 [54] decreases induction and progression of EAE by reducing monocyte infiltration in the spinal cord, or in the eye, respectively, and that the receptor for CCL2, CCR2, is expressed on a subset of inflammatory monocytes that traffic to inflammation sites, playing a role in animal models of infection and atherosclerosis [55–57]. Thus, we hypothesize that blocking CCL2 expression could protect the visual pathway from ON-induced damage. Bindarit is a small, synthetic indazolic derivative that preferentially inhibits transcription of the monocyte chemoattractant subfamily of CC chemokines [58]. Through its ability to interfere with monocyte recruitment, bindarit has shown clinical efficacy in a broad array of experimental inflammatory, autoimmune, and vascular disorders [59–63]. It has been demonstrated that bindarit blocks LPS-induced CCL2 expression in the brain and spinal cord [45]. As shown herein, a single dose of bindarit co-injected with LPS that decreased CCL2 upregulation at 6 h post-injection, reduced functional (PLR) and structural (RGC number) consequences of ON at 21 days post-LPS, supporting that an early CCL2 upregulation plays a key role in optic nerve damage. Notwithstanding, since bindarit also blocks the expression of CCL7 and CCL8 [58], the involvement of these chemokines in ON-induced damage cannot be ruled out.

A relatively early treatment with etoposide or gadolinium chloride that decreased peripheral monocyte percentage up to 7 days post-injection also protected the PLR and RGC number from the damage induced by experimental ON at 21 days

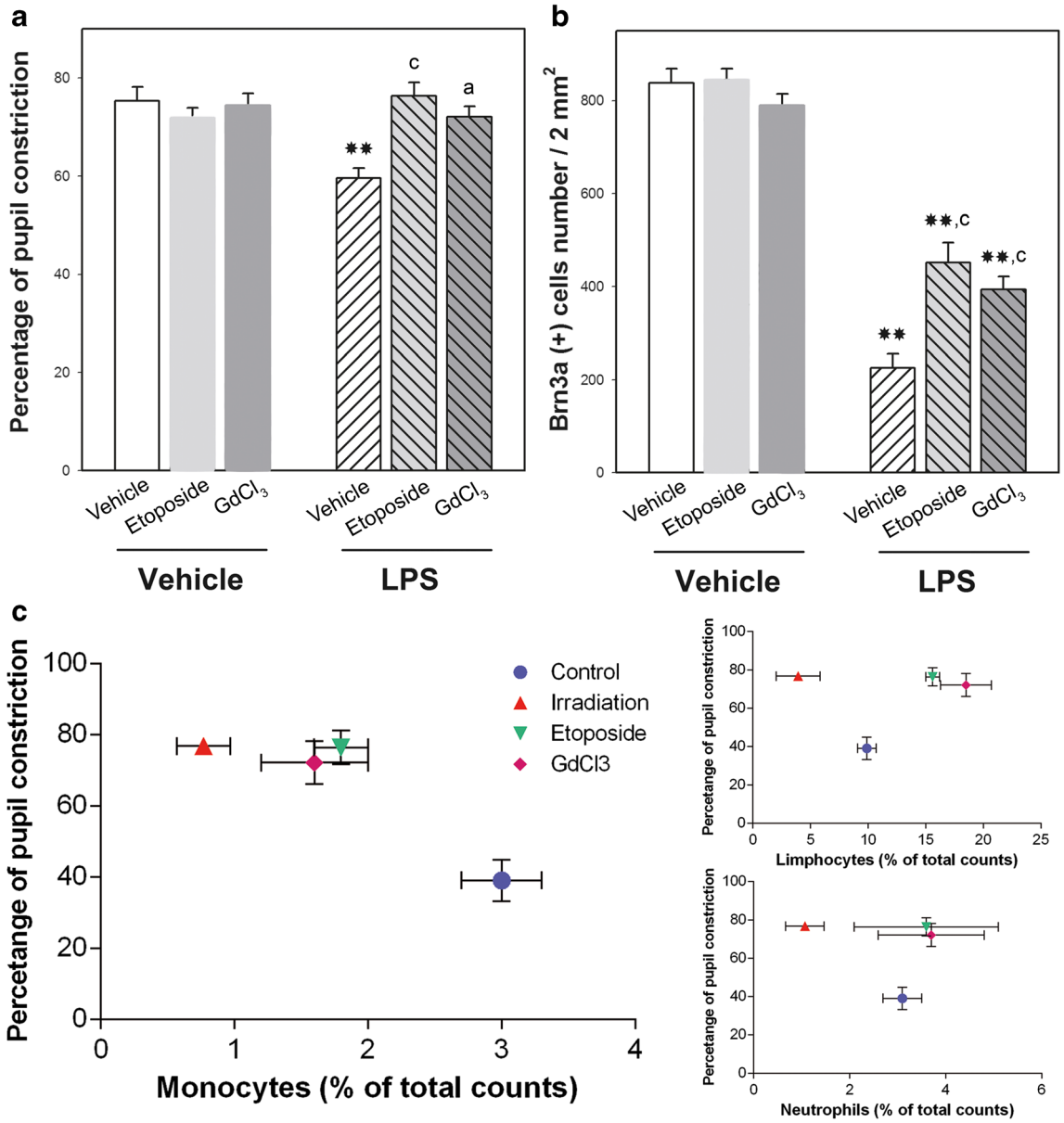

Fig. 8 Influence of monocytes on optic nerve damage induced by ON. Panels **A** and **B**: effect of etoposide and gadolinium chloride administration on PLR and RGC number at 21 days post-LPS, respectively. Etoposide and gadolinium chloride significantly prevented the effect of LPS on PLR and RGC number at 21 days post-injection. Panel **C**: correlation between monocyte, lymphocyte, and neutrophil percentage and the PLR at 7 days post-LPS. A negative relationship between the PLR and monocyte (but not lymphocyte or neutrophil) percentage was evident. Data are the mean ± SEM ($n = 5$ animals per group). Two-way ANOVA, *PLR*: $F_{interaction(1,16)}$, 17.22 $P < 0.001$; *Brn3a(+)*: $F_{interaction\ (1,16)}$, 11,56 $P < 0.01$. ** $P < 0.01$, vs. vehicle-injected optic nerves; a: < 0.05: c: $P < 0.001$ vs. LPS-injected optic nerves, by Tukey's test

post-LPS. In addition, a negative correlation between PLR and peripheral monocyte (but not lymphocyte and neutrophil) percentage in irradiated animals or animals treated with etoposide or gadolinium chloride at 7 days post-LPS further confirmed a key role of this cell type in visual pathway alterations induced by experimental ON. In agreement, it has been demonstrated that macrophage depletion in acute EAE leads to a complete suppression of clinical signs [10, 64]. At present, we do not have any explanation for the increase in neutrophil percentage induced by etoposide and gadolinium chloride at 21 days. However, a compensatory mechanism operating at 2 weeks after stopping these treatments cannot be ruled out.

It should be noted that the protection from RGC loss was not complete with any of the treatments explored herein. Therefore, it is reasonable to believe that a remnant monocyte infiltration even after these treatments or the occurrence of other mechanisms besides monocyte-mediated events, could

also contribute to RGC loss. At present, additional mechanisms leading to RGC damage in ON are being analyzed.

Understanding the timing and mechanisms of axonal injury and neuronal cell death induced by ON is important for developing potential neuroprotective therapies to prevent permanent vision loss. This study supports the following sequence of events at early stages of ON-induced by LPS: BBB disruption, neutrophil recruitment, CCL2 upregulation in neutrophils (later on in microglia/macrophages), and consequently, recruitment of monocytes, which seem to be key players in visual damage, as demonstrated herein through four different experimental strategies (irradiation, bindarit, etoposide, or gadolinium chloride treatments). Although the events that occur before and after these steps should be examined in detail, these results support the paradigm that primary ON is triggered by inflammatory events associated with an early monocyte infiltration. If correct, the manipulation of CCL2 expression or other strategies aimed at reducing monocyte recruitment into the optic nerve may prove effective against primary ON-induced visual loss.

Funding This work was supported by grants from the Agencia Nacional de Promoción Científica y Tecnológica (PICT 1563, PICT 2731), The University of Buenos Aires (20020130100564), and Consejo Nacional de Investigaciones Científicas y Técnicas (PIP 0707), Argentina. The funding organizations have no role in the design or conduct of this research.

Compliance with Ethical Standards

Conflict of Interest The authors declare that they have no conflict of interest.

Ethical Approval All animal procedures were in strict accordance with the ARVO Statement for the Use of Animals in Ophthalmic and Vision Research. The ethic committee of the School of Medicine, University of Buenos Aires (Institutional Committee for the Care and Use of Laboratory Animals, (CICUAL)) approved this study, and all efforts were made to minimize animal suffering.

Informed Consent Informed consent was obtained from all individual participants included in the study.

References

1. Toosy AT, Mason DF, Miller DH (2014) Optic neuritis. Lancet Neurol 13:83–99. https://doi.org/10.1016/S1474-4422(13)70259-X
2. Pau D, Al Zubidi N, Yalamanchili S, Plant GT, Lee AG (2011) Optic neuritis. Eye (Lond) 25:833–842. https://doi.org/10.1038/eye.2011.81
3. Kale N (2016) Optic neuritis as an early sign of multiple sclerosis. Eye Brain 8:195–202. https://doi.org/10.2147/EB.S54131
4. Aranda ML, Dorfman D, Sande PH, Rosenstein RE (2015) Experimental optic neuritis induced by the microinjection of lipopolysaccharide into the optic nerve. Exp Neurol 266:30–41. https://doi.org/10.1016/j.expneurol.2015.01.010
5. Jones KA, Maltby S, Plank MW, Kluge M, Nilsson M, Foster PS, Walker FR (2018) Peripheral immune cells infiltrate into sites of secondary neurodegeneration after ischemic stroke. Brain Behav Immun 67:299–307. https://doi.org/10.1016/j.bbi.2017.09.006
6. Kuo PC, Scofield BA, Yu IC, Chang FL, Ganea D, Yen JH (2016) Interferon-β modulates inflammatory response in cerebral ischemia. J Am Heart Assoc 5. doi: https://doi.org/10.1161/JAHA.115.002610.
7. Nguyen HX, Hooshmand MJ, Saiwai H, Maddox J, Salehi LA, Nishi RA, Salazar D, Uchida N et al (2017) Systemic neutrophil depletion modulates the migration and fate of transplanted human neural stem cells to rescue functional repair. J Neurosci 37:9269–9287. https://doi.org/10.1523/JNEUROSCI.2785-16.2017
8. Nourshargh S, Alon R (2014) Leukocyte migration into inflamed tissues. Immunity 41:694–707. https://doi.org/10.1016/j.immuni.2014.10.008
9. Aubé B, Lévesque SA, Paré A, Chamma É, Kébir H, Gorina R, Lécuyer MA, Alvarez JI et al (2014) Neutrophils mediate blood-spinal cord barrier disruption in demyelinating neuroinflammatory diseases. J Immunol 193:2438–2454. https://doi.org/10.4049/jimmunol.1400401
10. Hendriks JJ, Teunissen CE, de Vries HE, Dijkstra CD (2005) Macrophages and neurodegeneration. Brain Res Brain Res Rev 48:185–195. https://doi.org/10.1016/j.brainresrev.2004.12.008
11. Mishra MK, Yong VW (2016) Myeloid cells - targets of medication in multiple sclerosis. Nat Rev Neurol 12:539–551. https://doi.org/10.1038/nrneurol.2016.110
12. Shindler KS, Ventura E, Dutt M, Rostami A (2008) Inflammatory demyelination induces axonal injury and retinal ganglion cell apoptosis in experimental optic neuritis. Exp Eye Res 87:208–213. https://doi.org/10.1016/j.exer.2008.05.017
13. Adamus G, Brown L, Andrew S, Meza-Romero R, Burrows GG, Vandenbark AA (2012) Neuroprotective effects of recombinant T-cell receptor ligand in autoimmune optic neuritis in HLA-DR2 mice. Invest Ophthalmol Vis Sci 53:406–412. https://doi.org/10.1167/iovs.11-8419
14. Brambilla R, Dvoriantchikova G, Barakat D, Ivanov D, Bethea JR, Shestopalov VI (2012) Transgenic inhibition of astroglial NF-κB protects from optic nerve damage and retinal ganglion cell loss in experimental optic neuritis. J Neuroinflammation 9:213. https://doi.org/10.1186/1742-2094-9-213
15. Dorfman D, Aranda ML, González Fleitas MF, Chianelli MS, Fernandez DC, Sande PH, Rosenstein RE (2014) Environmental enrichment protects the retina from early diabetic damage in adult rats. PLoS One 9:e101829. https://doi.org/10.1371/journal.pone.0101829
16. Fernandez DC, Sande PH, Chianelli MS, Aldana Marcos HJ, Rosenstein RE (2011) Induction of ischemic tolerance protects the retina from diabetic retinopathy. Am J Pathol 178:2264–2274. https://doi.org/10.1016/j.ajpath.2011.01.040
17. Nakata W, Nakai Y, Yoshida T, Sato M, Hatano K, Nagahara A, Fujita K, Uemura M et al (2015) Bone marrow-derived cells contribute to regeneration of injured prostate epithelium and stroma. Prostate 75:806–814. https://doi.org/10.1002/pros.22962
18. Kim SY, Cheon SY, Kim EJ, Lee JH, Kam EH, Kim JM, Park M, Koo BN (2017) Isoflurane postconditioning inhibits tPA-induced matrix metalloproteinases activation after hypoxic injury via low-density lipoprotein receptor-related protein and extracellular signal-regulated kinase pathway. Neurochem Res 42:1533–1542. https://doi.org/10.1007/s11064-017-2211-2
19. Su EJ, Fredriksson L, Geyer M, Folestad E, Cale J, Andrae J, Gao Y, Pietras K et al (2008) Activation of PDGF-CC by tissue plasminogen activator impairs blood-brain barrier integrity during ischemic stroke. Nat Med 14:731–737. https://doi.org/10.1038/nm1787

20. Dong MX, Hu QC, Shen P, Pan JX, Wei YD, Liu YY, Ren YF, Liang ZH et al (2016) Recombinant tissue plasminogen activator induces neurological side effects independent on thrombolysis in mechanical animal models of focal cerebral infarction: a systematic review and meta-analysis. PLoS One 11:e0158848. https://doi.org/10.1371/journal.pone.0158848
21. Fredriksson L, Lawrence DA, Medcalf RL (2017) tPA modulation of the blood-brain barrier: a unifying explanation for the pleiotropic effects of tPA in the CNS. Semin Thromb Hemost 43:154–168. https://doi.org/10.1055/s-0036-1586229
22. Reijerkerk A, Kooij G, van der Pol SM, Leyen T, van Het Hof B, Couraud PO, Vivien D, Dijkstra CD et al (2008) Tissue-type plasminogen activator is a regulator of monocyte diapedesis through the brain endothelial barrier. J Immunol 181:3567–3574. https://doi.org/10.4049/jimmunol.181.5.3567
23. Yepes M, Sandkvist M, Moore EG, Bugge TH, Strickland DK, Lawrence DA (2003) Tissue-type plasminogen activator induces opening of the blood-brain barrier via the LDL receptor-related protein. J Clin Invest 112:1533–1540. https://doi.org/10.1172/JCI19212
24. Puliti M, von Hunolstein C, Bistoni F, Castronari R, Orefici G, Tissi L (2002) Role of macrophages in experimental group B streptococcal arthritis. Cell Microbiol 4:691–700. https://doi.org/10.1046/j.1462-5822.2002.00223.x
25. Pendino KJ, Meidhof TM, Heck DE, Laskin JD, Laskin DL (1995) Inhibition of macrophages with gadolinium chloride abrogates ozone-induced pulmonary injury and inflammatory mediator production. Am J Respir Cell Mol Biol 13:125–132. https://doi.org/10.1165/ajrcmb.13.2.7542894
26. Prinz M, Priller J (2017) The role of peripheral immune cells in the CNS in steady state and disease. Nat Neurosci 20:136–144. https://doi.org/10.1038/nn.4475
27. Hu P, Pollard J, Hunt N, Chan-Ling T (1998) Microvascular and cellular responses in the retina of rats with acute experimental allergic encephalomyelitis (EAE). Brain Pathol 8:487–498. https://doi.org/10.1111/j.1750-3639.1998.tb00169
28. Park HJ, Shin JY, Kim HN, Oh SH, Song SK, Lee PH (2015) Mesenchymal stem cells stabilize the blood-brain barrier through regulation of astrocytes. Stem Cell Res Ther 6:187. https://doi.org/10.1186/s13287-015-0180-4
29. Liu Y, Xie X, Xia LP, Lv H, Lou F, Ren Y, He ZY, Luo XG (2017) Peripheral immune tolerance alleviates the intracranial lipopolysaccharide injection-induced neuroinflammation and protects the dopaminergic neurons from neuroinflammation-related neurotoxicity. J Neuroinflammation 14:223. https://doi.org/10.1186/s12974-017-0994-3
30. Brown DA, Sawchenko PE (2007) Time course and distribution of inflammatory and neurodegenerative events suggest structural bases for the pathogenesis of experimental autoimmune encephalomyelitis. J Comp Neurol 502:236–260. https://doi.org/10.1002/cne.21307
31. Banks WA, Erickson MA (2010) The blood-brain barrier and immune function and dysfunction. Neurobiol Dis 37:26–32. https://doi.org/10.1016/j.nbd.2009.07.031
32. Jaworowicz DJ Jr, Korytko PJ, Singh Lakhman S, Boje KM (1998) Nitric oxide and prostaglandin E2 formation parallels blood-brain barrier disruption in an experimental rat model of bacterial meningitis. Brain Res Bull 46:541–546
33. Aranda ML, González Fleitas MF, De Laurentiis A, Keller Sarmiento MI, Chianelli M, Sande PH, Dorfman D, Rosenstein RE (2016) Neuroprotective effect of melatonin in experimental optic neuritis in rats. J Pineal Res 60:360–372. https://doi.org/10.1111/jpi.12318
34. Aranda ML, González Fleitas MF, Dieguez HH, Milne GA, Devouassoux JD, Keller Sarmiento MI, Chianelli M, Sande PH et al (2019) Therapeutic benefit of environmental enrichment on optic neuritis. Neuropharmacology 145:87–98. https://doi.org/10.1016/j.neuropharm.2017.12.017
35. Siao CJ, Fernandez SR, Tsirka SE (2003) Cell type-specific roles for tissue plasminogen activator released by neurons or microglia after excitotoxic injury. J Neurosci 23:3234–3242. https://doi.org/10.1523/JNEUROSCI.23-08-03234.2003
36. Villarán RF, de Pablos RM, Argüelles S, Espinosa-Oliva AM, Tomás-Camardiel M, Herrera AJ, Cano J, Machado A (2009) The intranigral injection of tissue plasminogen activator induced blood-brain barrier disruption, inflammatory process and degeneration of the dopaminergic system of the rat. Neurotoxicology 30:403–413. https://doi.org/10.1016/j.neuro.2009.02.011
37. Baron A, Montagne A, Cassé F, Launay S, Maubert E, Ali C, Vivien D (2010) NR2D-containing NMDA receptors mediate tissue plasminogen activator-promoted neuronal excitotoxicity. Cell Death Differ 17:860–871. https://doi.org/10.1038/cdd.2009.172
38. Tsirka SE, Gualandris A, Amaral DG, Strickland S (1995) Excitotoxin-induced neuronal degeneration and seizure are mediated by tissue plasminogen activator. Nature 377:340–344. https://doi.org/10.1038/377340a0
39. You Y, Gupta VK, Li JC, Klistorner A, Graham SL (2013) Optic neuropathies: characteristic features and mechanisms of retinal ganglion cell loss. Rev Neurosci 24:301–321. https://doi.org/10.1515/revneuro-2013-0003
40. Howell GR, Soto I, Zhu X, Ryan M, Macalinao DG, Sousa GL, Caddle LB, MacNicoll KH et al (2012) Radiation treatment inhibits monocyte entry into the optic nerve head and prevents neuronal damage in a mouse model of glaucoma. J Clin Invest 122:1246–1261. https://doi.org/10.1172/JCI61135
41. Mahad DJ, Ransohoff RM (2003) The role of (MCP-1) CCL2 and CCR2 in multiple sclerosis and experimental autoimmune encephalomyelitis (EAE). Semin Immunol 15:23–32. https://doi.org/10.1016/S1044-5323(02)00125-2
42. Hickman SE, El Khoury J (2010) Mechanisms of mononuclear phagocyte recruitment in Alzheimer's disease. CNS Neurol Disord Drug Targets 9:168–173. https://doi.org/10.2174/187152710791011982
43. Babcock AA, Kuziel WA, Rivest S, Owens T (2003) Chemokine expression by glial cells directs leukocytes to sites of axonal injury in the CNS. J Neurosci 23:7922–7930. https://doi.org/10.1523/JNEUROSCI.23-21-07922.2003
44. Fuentes ME, Durham SK, Swerdel MR, Lewin AC, Barton DS, Megill JR, Bravo R, Lira SA (1995) Controlled recruitment of monocytes and macrophages to specific organs through transgenic expression of monocyte chemoattractant protein-1. J Immunol 155:5769–5776
45. Ge S, Shrestha B, Paul D, Keating C, Cone R, Guglielmotti A, Pachter JS (2012) The CCL2 synthesis inhibitor bindarit targets cells of the neurovascular unit, and suppresses experimental autoimmune encephalomyelitis. J Neuroinflammation 9:171. https://doi.org/10.1186/1742-2094-9-171
46. Yadav A, Saini V, Avora S (2010) MCP-1: chemoattractant with a role beyond immunity: a review. Clin Chim Acta 411:1570–1579. https://doi.org/10.1016/j.cca.2010.07.006
47. Zhang L, Ma P, Guan Q, Meng L, Su L, Wang L, Yuan B (2018) Effect of chemokine CC ligand 2 (CCL2) on α-synuclein-induced microglia proliferation and neuronal apoptosis. Mol Med Rep. https://doi.org/10.3892/mmr.2018.9468
48. Chang SL, Huang W, Mao X, Sarkar S (2017) NLRP12 inflammasome expression in the rat brain in response to LPS during morphine tolerance. Brain Sci 7(2):14. https://doi.org/10.3390/brainsci7020014
49. Davis RL, Stevens CW, Thomas Curtis J (2017) The opioid antagonist, β-funaltrexamine, inhibits lipopolysaccharide-induced neuroinflammation and reduces sickness behavior in mice. Physiol Behav 173:52–60. https://doi.org/10.1016/j.physbeh.2017.01.037

50. Le Thuc O, Cansell C, Bourourou M, Denis RG, Stobbe K, Devaux N, Guyon A, Cazareth J et al (2016) Central CCL2 signaling onto MCH neurons mediates metabolic and behavioral adaptation to inflammation. EMBO Rep 17:1738–1752. https://doi.org/10.15252/embr.201541499
51. Van Hove I, Lefevere E, De Groef L, Sergeys J, Salinas-Navarro M, Libert C, Vandenbroucke R, Moons L (2016) MMP-3 deficiency alleviates endotoxin-induced acute inflammation in the posterior eye segment. Int J Mol Sci 17. doi:https://doi.org/10.3390/ijms17111825
52. Arruda-Silva F, Bianchetto-Aguilera F, Gasperini S, Polletti S, Cosentino E, Tamassia N, Cassatella MA (2017) Human neutrophils produce CCL23 in response to various TLR-agonists and TNFα. Front Cell Infect Microbiol 7:176. https://doi.org/10.3389/fcimb.2017.00176
53. Huang DR, Wang J, Kivisakk P, Rollins BJ, Ransohoff RM (2001) Absence of monocyte chemoattractant protein 1 in mice leads to decreased local macrophage recruitment and antigen-specific T helper cell type 1 immune response in experimental autoimmune encephalomyelitis. J Exp Med 193:713–726. https://doi.org/10.1084/jem.193.6.713
54. Adamus G, Manczak M, Machnicki M (2001) Expression of CC chemokines and their receptors in the eye in autoimmune anterior uveitis associated with EAE. Invest Ophthalmol Vis Sci 42:2894–2903
55. Geissmann F, Jung S, Littman DR (2003) Blood monocytes consist of two principal subsets with distinct migratory properties. Immunity 19:71–82. https://doi.org/10.1016/S1074-7613(03)00174-2
56. Serbina NV, Pamer EG (2006) Monocyte emigration from bone marrow during bacterial infection requires signals mediated by chemokine receptor CCR2. Nat Immunol 7:311–317. https://doi.org/10.1038/ni1309
57. Tacke F, Alvarez D, Kaplan TJ, Jakubzick C, Spanbroek R, Llodra J, Garin A, Liu J et al (2007) Monocyte subsets differentially employ CCR2, CCR5, and CX3CR1 to accumulate within atherosclerotic plaques. J Clin Invest 117:185–194. https://doi.org/10.1172/JCI28549
58. Mirolo M, Fabbri M, Sironi M, Vecchi A, Guglielmotti A, Mangano G, Biondi G, Locati M et al (2008) Impact of the anti-inflammatory agent bindariton the chemokinome: selective inhibition of the monocytechemoattractant proteins. Eur Cytokine Netw 19:119–122. https://doi.org/10.1684/ecn.2008.0133
59. Bhatia M, Ramath RD, Chevali L, Guglielmotti A (2005) Treatment with bindarit, ablocker of MCP-1 synthesis, protects mice against acute pancreatitis. Am J Physiol Gastrointest Liver Physiol 288:G1259–G1265. https://doi.org/10.1152/ajpgi.00435
60. Grassia G, Maddaluno M, Guglielmotti A, Mangano G, Biondi G, Maffia P, Ialenti A (2009) The anti-inflammatory agent bindarit inhibits neointima formation in both rats and hyperlipodaemic mice. Cardiovasc Res 84:485–493. https://doi.org/10.1093/cvr/cvp238
61. Guglielmotti A, Aquilini L, D'Onofrio F, Rosignoli MT, Milanese C, Pinza M (1998) Bindarit prolongs survival and reduces renal damage in NZB/W lupus mice. Clin Exp Rheumatol 16:149–154
62. Guglielmotti A, D'Onofrio E, Coletta I, Aquilini L, Milanese C, Pinza M (2002) Amelioration of rat adjuvant arthritis by therapeutic treatment with bindarit, an inhibitor of MCP-1 and TNF-alpha production. Inflamm Res 51:252–258
63. Lin J, Zhu X, Chade A, Jordan KL, Lavi R, Daghini E, Gibson ME, Guglielmotti A et al (2009) Monocyte chemoattractant proteins mediate microvascular dysfunction in swine renovascular hypertension. Arterioscler Thromb Vasc Biol 29:1810–1816. https://doi.org/10.1161/ATVBAHA.109.190546
64. Huitinga N, van Rooijen CJ, De Groot CJ, Uitdehaag BM, Dijkstra CD (1990) Suppression of experimental allergic encephalomyelitis in Lewis rats after elimination of macrophages. J Exp Med 172:1025–1033. https://doi.org/10.1084/jem.172.4.1025